Cooper-minimum effects in the photoionization cross sections of 4*d* and 5*d* electrons in solid compounds

G. Rossi and I. Lindau
Stanford Electronics Laboratories, Stanford University, Stanford, California 94305

L. Braicovich and I. Abbati
Istituto di Fisica del Politecnico, I-20133 Milano, Italy
(Received 22 February 1983)

We present experimental determinations of the cross section for photoionization for 4*d* and 5*d* valence states in transition and noble metals and at the interfaces that these metals form with elemental semiconductors (group IV) in the photon-energy range $h\nu = 70-200$ eV. A description of the technique used to obtain cross sections σ from photoemission measurements is provided, and a phenomenological discussion of the strong dependence of σ on the distortion of the initial-state *d* wave function in the solid environment with respect to the atomic case and in solid-state compounds with respect to pure metals is proposed. A strong reflection of the chemistry involving the *d* states on the photoionization probability is found, in particular, at the Cooper minimum. The use of photoemission at the Cooper minimum to study interfaces and compounds involving 4*d* and 5*d* states is discussed with the support of data relevant to commonly investigated systems, as well as an application to a less-studied refractory-metal—Si interface, namely, Mo/Si.

I. INTRODUCTION

The photoionization process is governed by a probability function which depends on the absorption cross section but is also characteristic of the particular initial and final states involved in the electron emission which is called (partial) photoionization cross section. The Cooper-minimum (CM) effect is a minimum in the photoionization cross section for particular orbitals (initial-state wave functions) and particular excitation energies (final-state wave functions). The presence of Cooper minima in 4*d* and 5*d* orbitals was predicted[1-3] on the basis of the presence of a node in the radial part of the 4*d* and 5*d* atomic wave functions (see discussion). With the advent of synchrotron radiation as a suitable source of monochromatic light over the vacuum ultraviolet (vuv) and soft x-ray energy ranges, the measurements of the photoionization cross section of electronic subshells became feasible, both at the atomic (gas phase) and solid states.[4-11]

While atomic photoionization cross-section (σ) calculations for *d* orbitals ($n > 3$) (Refs. 3, 10, and 12) show modulations of 2 orders of magnitude between maxima and minima, the measurements at the solid state for (*d*) valence subshells show smaller effects, typically 1 order of magnitude smaller. Only on the basis of the recent characterizations of all the experimental and physical variables involved in the measurements of σ in solids (see Sec. III and Ref. 13), highly reliable data on the Cooper minimum in 4*d* and 5*d* solids are appearing in the literature allowing the discussion of the solid-state effects on the σ.[9,10] The nature of the solid-state effects on σ (in the $h\nu$ range 70—200 eV) is discussed in this paper in connection with the chemically induced changes in the 4*d* and 5*d* initial-state wave functions in transition-metal—semiconductor (group IV) compounds, alloys, and interfaces.

This paper is organized into the following sections. Section II deals with the experimental setup for our measurements of σ in solids and the preparation and measurements of Si- (Ge-) metal interfaces. Section III is devoted to a thorough description of the method used to obtain σ measurements from photoemission intensity measurements in solids. The definition of the experimental σ^* is given and all the correction factors are discussed. In the second part of the paper, we present results for σ of 4*d*, 5*d*, and *sp* subshells over the photon-energy range $h\nu = 70-200$ eV for Ag/Si, Pd_2Si, and Au/Si, and compare them to the σ measured for pure Ag, Pd, and Au solids (Sec. IV). Spectra of valence-band (VB) energy-distribution curves (EDC's) in and out of the CM are given and discussed indicating the changes in the σ as a consequence of changes in the initial states. In the last part of the paper (Sec. V), we define the use of $h\nu$-dependent photoemission as a powerful tool to study the chemical bond in solids and show a remarkable application of σ measurements to the Si/Mo interface.

II. EXPERIMENTAL TECHNIQUES

The photoemission and σ measurements presented in this paper have been obtained in several experiments using the same ultrahigh-vacuum apparatus[14] and type of electron energy analyzer [cylindrical mirror analyzer (CMA)],[15] described previously in the literature and, as an excitation source, monochromatic synchrotron radiation on the 4° beam line equipped with a "grasshopper" monochromator at the Stanford Synchrotron Radiation Laboratory (SSRL).[16,17] The light beam enters the experimental chamber at an angle of 105° with respect to the CMA axis,

and the sample sits in the common focus of the CMA and the light beam. The σ measurements were obtained mostly with the sample surfaces making an angle of $\sim 50°$ to the beam for reasons explained in detail in Sec. III, but also slightly different angles and 15° incident angles were employed. The EDC's from the semiconductor-metal interfaces were all obtained with 15° light incidence.

The intensity of the monochromatic beam was monitored by a total electron yield detector collecting the emission of an Au- or Cu-coated highly transparent net placed in between the monochromator and the experimental chamber.

The sample preparation was done *in situ* (base pressure 5×10^{-11} Torr) by cleaving Si(111)-oriented rods and evaporating the metals with techniques previously described.[18–21] The pure metal films were obtained by evaporation of 100–300 Å of material onto clean stainless-steel substrates.

III. THE DETERMINATION OF THE EXPERIMENTAL σ

The relevant quantity which is the object of the present research is the modulation of the cross section for photoionization σ in the photon-energy range 70–200 eV (shape of the σ function). Therefore, the data are plotted in relative units (arbitrary) and are not calibrated on an absolute Mb scale. The uncertainty connected with an absolute calibration of the experimental data would be considerable because of the lack of knowledge of the exact number of photons/cm^2 sec provided by the light source and the approximations in the absolute values of some of the correction factors to be applied to the data (i.e., the escape depths). The trends of these quantities, on the other hand, have been carefully measured and the resulting curves (see discussion below) have been applied to the raw data to yield highly reliable σ curves. Cross-section curves for different substances were measured in different experiments with, in some cases, differences in the geometric factors involved in the measurement. Therefore, the comparison between the σ obtained for different substances must take into account that the magnitudes may not be strictly comparable.

The quantity measured in the experiment is the intensity of the photoelectron yield for the chosen electron states at different photon energies. We have measured the entire valence band EDC's at $h\nu$ values covering the (70–200)-eV range (spacing of 5 or 10 eV) and then calculated the areas under the considered peaks. This technique is more time consuming than the constant–initial-state spectrometry (CIS) technique but allows a careful subtraction of the emission from the valence states and, therefore, gives a more precise estimate of the photoemission intensity due to the chosen subshell.

The measured intensity obviously depends on the brightness of the light source so that it is sensitive to changes of the current and focusing of the stored electron beam in the synchrotron and on the position of the beam with respect to the deflecting mirror at the origin of the beam line. Owing to the imperfect reproducibility of this geometric factor for different electron injections in the synchrotron, all the data points for a given σ were obtained with the same beam and some data points were measured several times as the store beam was decaying. The correction for the beam current was done assuming the intensity of the synchrotron radiation linearly proportional to the stored current. Typical variation of the beam current over the time of the complete measurement of each σ were of -20%.

The photoelectron signal was detected with a cylindrical mirror analyzer with partial angular integration in counting mode. Therefore, from here on, we will refer to the intensity as the counting rate C.

Disregarding the solid-angle factor and the atomic density of our samples, since we express σ in arbitrary units, and assuming a thick photoemitter and an attenuation length for the light in the sample much larger than the photoelectron escape depth, as is the case in our experiments, the counting rate C (normalized to the beam current) is connected to the cross section σ by

$$C(h\nu)\propto\sigma(h\nu)L(E')\zeta(E_K)\Phi(h\nu)F(X,n,K,L)\ , \qquad (1)$$

where L is the photoelectron escape depth which depends on $h\nu$ through the dependence of the final-state energy E' above the Fermi level (kinetic energy of the photoelectron); $\zeta(E_K)$ is the efficiency of the photoelectron detector versus the kinetic energy of the photoelectrons; this function is characteristic of the detector used (here a CMA) and its operation mode (see below); $\Phi(h\nu)$ is the relative photon flux arriving onto the sample from the light source (synchrotron brightness and optical devices throughput). The function $F(X,n,K,L)$ describes the variations of effective photoexcitation of the sample due to reflection at the sample surface (loss of photons) and refraction of the light (changes of the light intensity within the photoelectron escape depth L). The theory of F has been developed in detail by Henke[22]; the reader is referred to that work for the description of the dependence of F on the angle of incidence of the light X, the index of refraction $(n+ik)$ of the sample, and L. For geometries that reduce the reflectivity-refractivity effects, F tends to unity and the formula (1) becomes simple and intuitive.

Owing to the finite resolution of the monochromator and of the electron analyzer, the exact formula would require the convolution of $\Phi(h\nu)$ and $\zeta(E_k)$ instead of their product. Actually, the accuracy of our measurements of σ is limited by the uncertainty of Φ, which amounts to $\pm15\%$ and, therefore, smaller errors are intentionally disregarded to benefit the simplicity of formula (1) and its intuitive value.

The application of (1) to analyze our data corresponds to the *empirical definition of the effective* σ in the present experiment. This σ must not be identified with the differential cross section; it is connected to this quantity via an integration over the angles, including the asymmetry parameter.[23] This fact must be taken into account when comparing our data with theoretical calculations but is not relevant for our phenomenological discussion. We, nevertheless, stress that the effect of such integration is not strong as it can be estimated by combining the results of Ref. 23 with the compiled atomic cross sections.[12] For-

mula (1) can be reversed

$$\sigma^* = \sigma F = \frac{C}{L\zeta\Phi} = CG \ , \tag{2}$$

where

$$G = \frac{1}{L\zeta\Phi} \ . \tag{3}$$

The cross section σ^* is not corrected for the optical effects (F) and G is the experimental correction factor. The remaining part of this section is devoted to the evaluation of G and to the connection between σ^* and σ.

A. The experimental corrections

The factor G depends on three functions which are discussed separately.

(1) The relative photon flux was obtained by measuring the total quantum yield versus $h\nu$ of two known absorbers, Au and Cu, and correcting the measured quantity for the optical absorption coefficients for those materials and for the relative intensities of higher-order light frequencies throughput by the monochromator. The intensity of second-order light in the $h\nu$ range 50–100 eV is of the same order of magnitude as the first order and can therefore contribute as much as 60% to the total yield of Au or Cu. The relative intensities of second and third order with respect to first-order light for the grasshopper monochromator used in our experiment have been measured by Hecht *et al.*[17] The Φ resulting after the corrections is plotted in Fig. 1; the shape of the curve is analogous to that previously given in Ref. 23 for the same beam line.

(2) The electron escape depth varies only slightly in the energy range of our measurements. The dependence of L on the kinetic energy has been taken from the escape-depth compilation of Ref. 24. The relative values of the $L(E)$ function were used in our σ (since it is expressed in arbitrary units), avoiding the absolute values of $L(E')$, which is important when the $L(E')$ curve is applied to the Si-metal compounds. Recent escape-depth determinations for Pd_2Si, for example,[25] give a value of 8.4 Å for $E_k \cong 90$ eV, which is a higher value than commonly accepted or deduced by applying quantitatively the universal $L(E')$ curve.[26]

In our experiment, we have studied shallow electron levels (valence band) with photon energies much higher than the binding energies of the initial-state electrons. It is then possible to assume $L(E') \simeq L(h\nu)$ obtaining an escape-depth correction which is the same at constant $h\nu$, for all the substances investigated.

(3) The CMA efficiency ζ depends on the electrostatic configuration of the analyzer, which is determined by the particular operation mode. We operated the CMA in two modes: in the "retarding" mode, where a constant pass energy is set and the efficiency should be proportional to $E_{\text{pass}}/E_{\text{kinetic}}$. In another mode, the CMA was operated with a computer, according to theoretical predictions by Palmberg,[15] in such a way as to give constant luminosity versus E_k. We have measured the counting rate $C(h\nu)$ for Pd $4d$ in both modes. The ratio of the counting rates in the two cases is proportional to $1/E_k$, thus confirming the statement that the efficiency ζ_{CMA} in the retarding mode varies as $1/E_k$ within the experimental accuracy. For the same reason as in point (2), we approximate $\zeta(E_k) \simeq \zeta(h\nu)$. Most of the data were taken in the retarding mode in order to compare our data directly with counting rates from the literature and with our previous results.

By combining the above results on Φ, L, and ζ, we obtain the cumulative correction factor G (plotted in Fig. 2) which transforms, by multiplication, the counting rate C into the cross section σ^*. The overall accuracy of G is

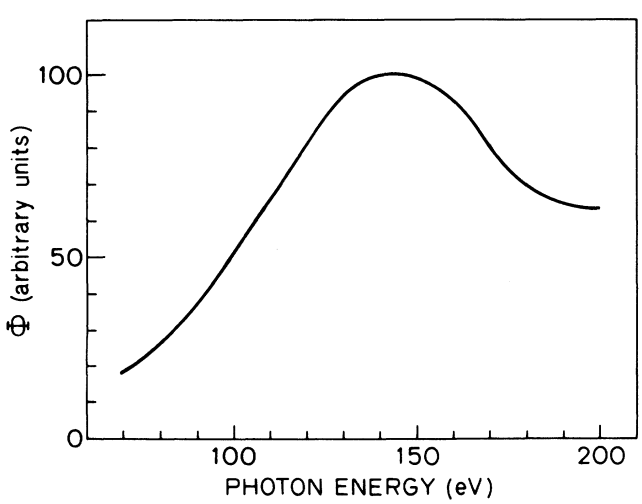

FIG. 1. Photon output characteristic for the 4° grasshopper beam line at SSRL in the range $h\nu = 70$–200 eV (see text).

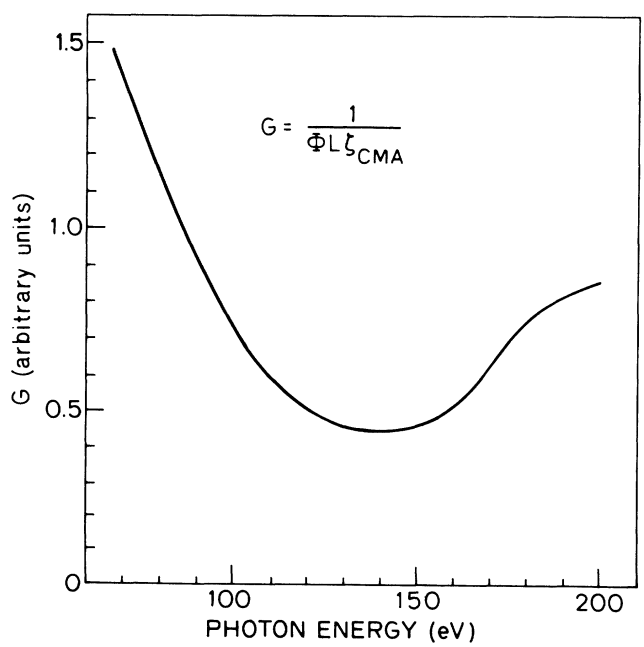

FIG. 2. Correction factor G to transform counting rates C to cross sections σ for photoemission data obtained with a CMA and with the flux Φ of Fig. 1 (see text).

such that the final σ^* are accurate within $\pm 15\%$. This is due mostly to the uncertainty of the measurement of Φ and must be regarded as the upper limits of unknown systematic errors. The high values of C over the entire range explored reduce the statistical errors to a negligible factor. The overall accuracy of our measurements can be considered very satisfactory, and it is largely sufficient for the present discussion.

B. The connection of σ^* with σ

If the C measurements are done at a fixed incidence angle χ, the evaluation of the correction F requires the knowledge of the complex index of refraction of the substance over the entire $h\nu$ range of interest. In the case of most compounds, such information is not available and our strategy was to avoid the need for this correction by working at near-normal incidence, where F tends to unity in the soft x-ray spectrum. This allows us to consider $\sigma^* \cong \sigma$ with a high degree of confidence, as we tested in some cases by checking the insensitivity of the C on χ for different near-normal incidence experimental geometries.

Since in many of the synchrotron radiation photoemission experiments not specifically designed for cross-section research the grazing incidence of the light is employed, we have also carried out measurements at 15° of incidence (the same geometry of our previous experiments on interfaces) in order to compare σ with σ^*. We report in Fig. 3 the counting rate C in arbitrary units versus $h\nu$ at near-normal incidence and at grazing incidence of the light on the sample surface; the difference between the two curves which have been normalized arbitrarily to the same value at $h\nu = 150$ eV, a value for which the F correction is small, is due to optical effects. The maximum C at grazing incidence is lower by $\sim 45\%$, due to a loss of excitation of the sample due to reflection of part of the photons at the surface. The effect of the factor F for data taken at grazing incidence is large and as a result it is impossible to compare σ^* and σ on a quantitative basis; Figure 3 nevertheless shows that σ^* and σ can be *qualitatively* compared since their shapes are clearly analogous. With these precautions in mind, it is possible to use σ^* data obtained from experiments in which the optical corrections could not be directly evaluated.

A final remark on Fig. 3 is that both the counting rate curves show clearly the Cooper minimum of Pd at ~ 130 eV, i.e., even before the application of the correction factor G discussed above. The Cooper minimum for $4d$ elements is generally already seen in the raw data.

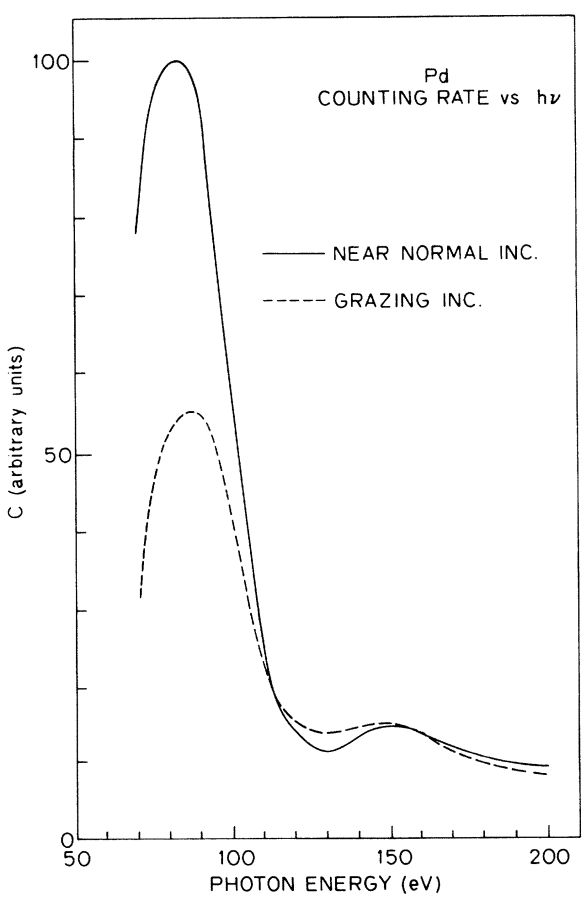

FIG. 3. Pd $4d$ emission intensity as measured at near-normal incidence of the light on the sample surface (solid line) or at grazing incidence (dashed curve). The curves are normalized at the same value at $h\nu = 160$ eV and show directly the effect of loss of excitation of the sample due to the large reflection of photons at the low angles of incidence.

IV. RESULTS AND DISCUSSION

The Cooper-minimum effect in the atomic photoionization cross sections arises from the presence of a node in the radial portion of the initial-state wave function of several subshells (e.g., $4d$ and $5d$) and the consequent cancellation of the matrix elements for electron transitions to particular final states. For a given set of final states, the Cooper-minimum effect depends therefore on the particular shape of the initial-state wave function. The atomic $4d$ and $5d$ wave functions are such that Cooper minima are present for photoelectron final states corresponding to transitions excited by photon energies in the range $h\nu = 130-180$ eV.[1-3]

The Cooper minimum (in general, the photoionization cross section) is therefore expected to undergo solid-state effects because of the distortion of the initial-state wave function which is particularly strong for valence subshells. In general, a smaller Cooper effect is observed in solids.[9]

A particular solid-state situation is the formation of states in the valence band which are generated by the interaction of different electron states of the same energy (hereafter called hybridized orbitals) that maintain a dominant orbital character. Typical cases of hybridization of this kind are the $4d$-$3p$ and $5d$-$3p$ valence hybrids in transition-metal (d) silicon (p) compounds.

The effect of rehybridization on the d states in d-metal silicides is the formation of mixed orbitals of bonding and antibonding character redistributed on a wider energy range than the pure d states and the partial loss of d character.[27] Different amounts of rehybridization of the metal d states are present in different transition-metal—silicon (or germanium[28]) systems; the near-noble-metal silicides are characterized by a valence DOS dominated by the hybrid metal $4d$ ($5d$)—Si $3p$ band. Here we present two kinds

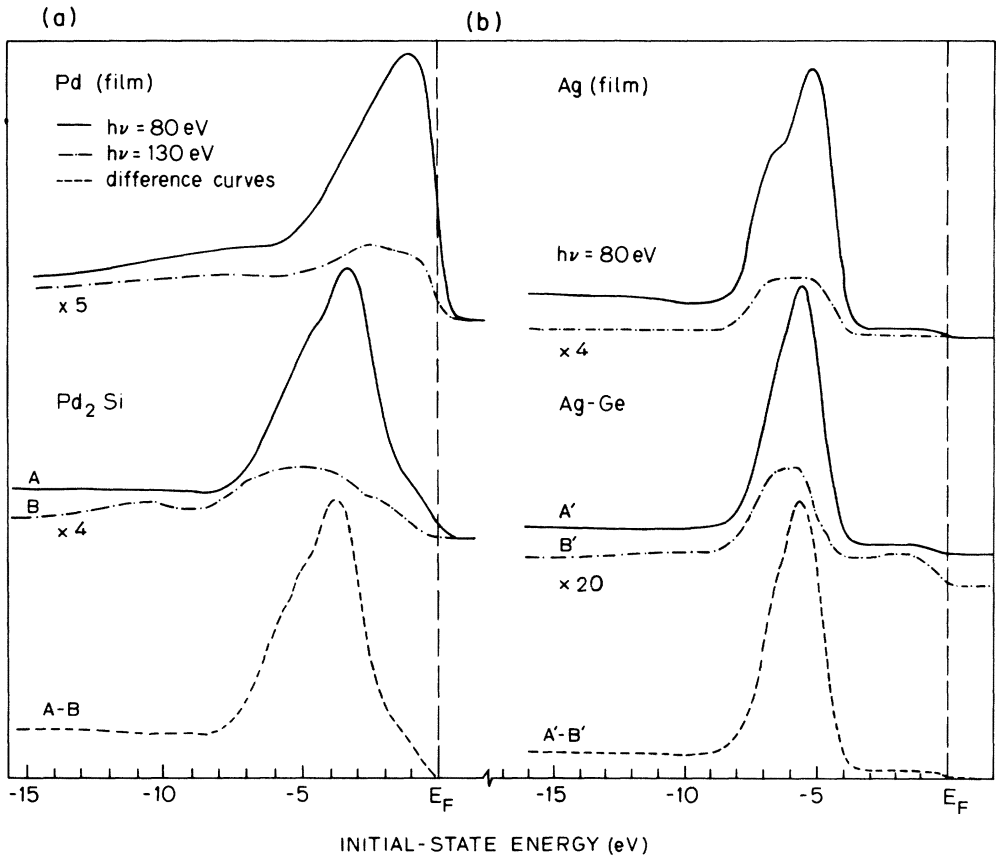

FIG. 4. Angle-integrated electron-energy distribution curves (EDC's) for 4*d* metals and 4*d*-metals—semiconductor interfaces: (a) Pd, Pd/Si (Pd_2Si) and (b) Ag, Ag/Ge. The solid curves correspond to EDC's obtained with $h\nu = 80$ eV in the high 4*d* cross section region, and the dotted-dashed curves are EDC's obtained at the Cooper minimum for 4*d* emission. The bottom curves (dashed) are the difference curves for Pd/Si and Ag/Ge obtained subtracting the Cooper-minimum spectra from the non-Cooper-minimum ones to give an indicator of the redistribution of the 4*d* states at the interface (see text).

of experimental results: angle-integrated photoemission valence energy distribution curves (EDC's) and photoionization cross-section curves for the $h\nu = 70$—200 eV range. From the EDC's, we learn the distribution of the electron states in the pure solids and in the compounds. This allows us to discuss the electronic structure of the samples whose cross sections we have measured. The EDC's for bulk crystalline Pd, Pt, Ag, and Au are presented in the top panels of Figs. 4 and 5, as obtained at two photon energies: $h\nu = 80$ eV, which corresponds to a very high cross-section value for the 4*d* and 5*d* states, so that the prominent features are all due to the emission from these states, and at $h\nu = 130$ and 150 eV that fall in the CM region where the *d* emission is greatly reduced.

Measured EDC's at the same energies for the interfaces that those metals form with Si or Ge at room temperature are displayed in the central curves of Figs. 4 and 5. The detailed discussion of the *d*-metal—semiconductor interfaces which these EFC's refer to has been previously published, and we refer the reader to the relevant papers. We will here summarize the main features of the electronic structure of these systems as an introduction to the discussion of the cross-section data which is the central part of the present work. The near-noble-metal—silicon interfaces in the left panel of Figs. 4 and 5 are characterized by a redistribution of the valence states, which involves both the metal *d* electrons and the *p* electrons of the semiconductor, with the formation of bonding states centered around -5.5-eV initial-state energy with respect to the Fermi level and antibonding states extending to the Fermi level. This new electron density of states (DOS) is directly observable in the EDC's of Figs. 4 and 5. Metal *d* states, which are less involved in the rehybridization with the Si 3*p* states determine the peak centered at -3.5 eV below E_F.

This is the electronic bonding configuration for Pd-Si and Pt-Si, which form interface compounds that have characteristics similar to those of the stable stoichiometric silicides.[29] In particular, the Pd/Si interface gives a reaction product that is strictly related to Pd_2Si, as was also proven recently by surface extended x-ray—absorption fine-structure (SEXAFS) measurements.[30] On the other hand, the noble metals Ag and Au do not form stable compounds with Si or Ge and the metal *d* states are slightly involved in the bonding configuration at the Ag/Ge (Ag/Si) interface or in the Au-Si alloy. In particular, for very low coverages, less than 0.3 monolayer (ML), Ag atoms are semi-isolated from each other and in weak interaction with the substrate at the Si or Ge surface,[19,31,32] so that the Ag 4*d* states for such coverages are expected to

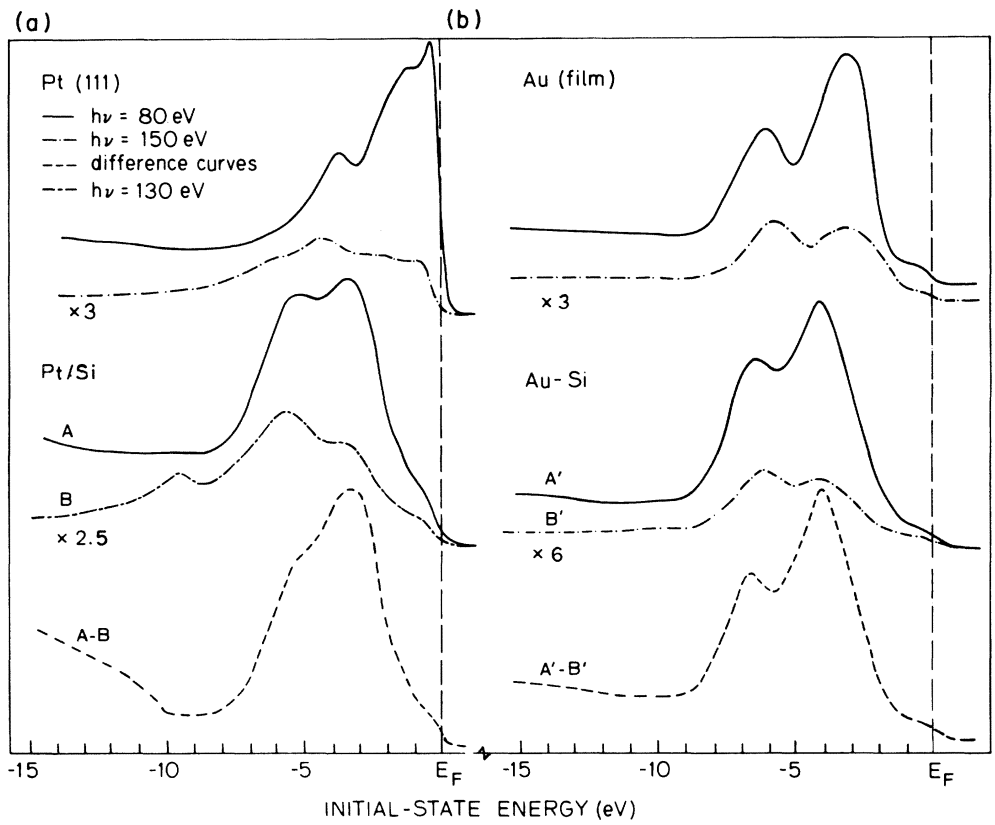

FIG. 5. Same as Fig. 4 for 5*d* metals and metal-silicon interfaces: (a) Pt, Pt/Si and (b) Au, Au/Si.

be more atomiclike than bandlike.[33] The Au/Si interface, instead, shows a high degree of intermixing without favorite composition of the relative alloy phases.[34,35] The bottom curves (dashed) of Figs. 4 and 5 will be discussed in Sec. V B.

The measured cross sections are presented in plots versus photon energy. The σ for the Ag 4*d* subshell for Ag metal (film) and for 0.3 ML of Ag on the Si(111) surface are given in Fig. 6. The σ for the Au 5*d* subshell for Au metal (film) and for the Au/Si interface as obtained by evaporating 6 ML of Au onto Si(111) at room temperature (RT) is given in Fig. 7; and the σ for the Pd 4*d* subshell in Pd metal and Pd/Si (Pd_2Si) interface are compared in Fig. 8. In all these plots, the σ for the *d* states in the metal and the interfaces are arbitrarily normalized to the same maximum value for graphical convenience.

Finally, we present, in Fig. 9, the σ for the total $n=3$ shell of Si (valence states). Before entering the discussion of the data, we want to remark that the whole 3*sp* valence band of Si has a much weaker and monotonic dependence on $h\nu$ in the considered energy range.

A quantitative comparison of the value of σ for Si and σ_{4d} or σ_{5d} is open to the difficulties discussed in Sec. III. It is, at present, only possible to state that at $h\nu=130-150$ eV (the CM region) the total $n=3$ shell σ of Si is of the same order of magnitude (within a factor of ± 1.5) of the 4*d*- or 5*d*-subshell σ for the metals, in rough agreement with Ref. 36.

All the 4*d*-subshell σ show a well-defined Cooper minimum. The localization of the *d* states in the solid preserves the effect although it is modified. The 5*d*-subshell σ for Au decreases rapidly beyond the maximum due to cancellation effects of the matrix elements, but there is no minimum as is the case for bulk Au.[7]

A. Comparison between the σ from hybridized and pure *d* orbitals

The comparison of the σ for a given valence subshell of an atomic species in different solid-state environments is particularly significant, since the initial-state wave function for valence states is directly modified by the chemistry. A correlation between the σ and the chemical configuration that involves *d* states in different compounds must then exist. To investigate this important point, we have also measured the σ for pure Ag, Au, and Pd (films).

The comparison between σ_{4d} for Ag and σ_{4d} for 0.3 ML of Ag onto Si(111) is done in Fig. 6 in a logarithmic representation to emphasize the changes in the CM region. The difference in the amplitude of the modulation of σ for the two cases is about one order of magnitude. The value at the CM of the σ_{4d} for the submonolayer Ag film on Si is smaller than at the maximum by a factor of 60. This is very close to the calculated CM for atomic Ag (the Hartree-Fock-Slater length approximation, Refs. 10 and 12) and therefore confirms the picture of semi-isolated Ag atoms for this low coverage. The pure Ag σ has a much weaker CM due to the much stronger solid-state effect.[9]

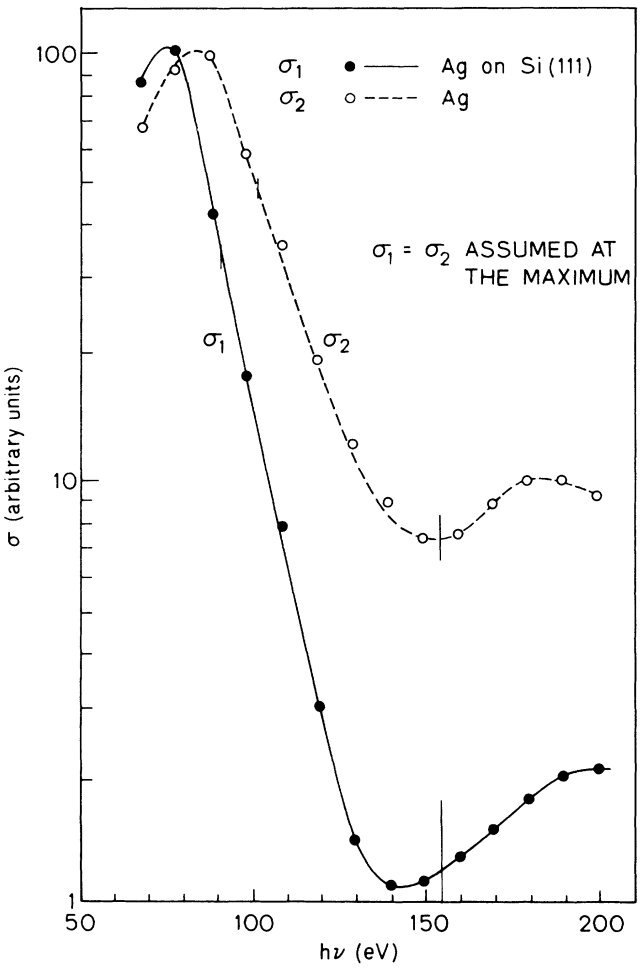

FIG. 6. Experimental photoionization cross sections σ for the $4d$ subshell of Ag in bulk Ag (thick film) (dashed line) and for semi-isolated Ag atoms corresponding to 0.3 ML deposited onto the Si(111) 2×1 surface (solid line). The two σ curves were arbitrarily normalized to the same value at the maximum for graphical convenience.

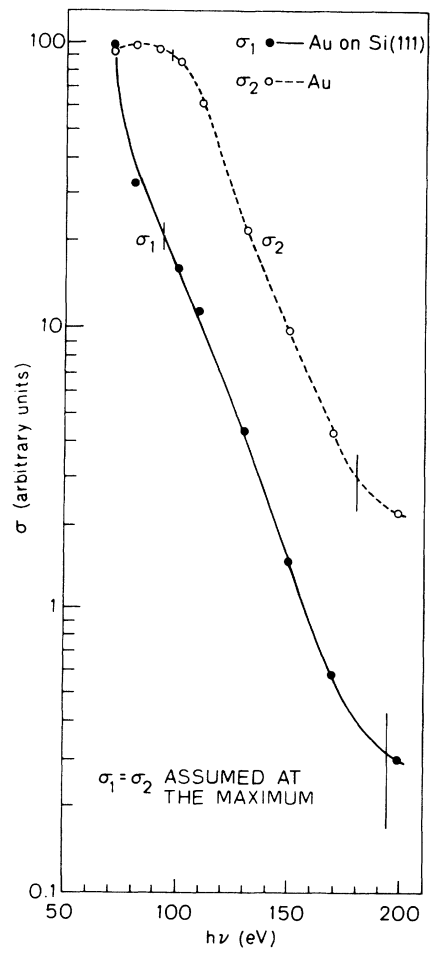

FIG. 7. Experimental σ for $5d$ subshell of Au in bulk Au (thick film) (dashed line) and for the Au/Si alloylike interface as obtained by evaporating 6 ML of Au onto the Si(111) 2×1 surface at room temperature.

Strong CM effects have been measured for core d levels [In $4d$, Sb $4d$,[23] and Xe $4d$ (Ref. 37)] in solids showing atomiclike modulations of σ. Core levels are much less distorted by the nonsperical crystal potential than valence states and their σ are not expected to deviate from the atomic ones other than for many-body effects. The distortion from atomiclike to bandlike valence states is therefore reflected by changes in the σ of *1 order of magnitude.*

A similar σ plot is obtained for Au $5d$ in solid Au and in the Au-Si mixed phase (Fig. 7). The modulation of σ for Au in Si is bigger than for the pure metal. Au diffused in Si cannot be considered by any means in an atomic state, but the overlapping between $5d$ states of Au atoms is greatly decreased due to the coordination of Au with mostly Si atoms,[34] also the d states are not heavily involved in the Au-Si alloy bonding configuration, as has been shown by photoemission experiments at the CM (see Fig. 10) and DOS calculations for Au_3Si.[35] The σ measurements clearly discriminate between these two solid but chemically different states for Au. The fact that no minimum is present in the measured σ, while a weak minimum was calculated by Goldberg *et al.* for atomic Au $5d$,[12] is probably a peculiar aspect of the solid-state effect on $5d$ orbitals and will not be discussed here, as well as the shift of the maximum of σ which in our measurements falls below our lower limit of $h\nu$.

The analysis of maxima and the onset of σ at the solid state is premature. More theory is needed on the effects of correlation,[38] both in the initial and final states that strongly affect these parts of σ. We only note that in the single-particle calculation[12] σ decreases monotonically above 40.8 eV. The shift that we observe for the maximum of σ in Au-Si towards lower $h\nu$ could be tentatively correlated to the smaller band character of the $5d$ states.

We finally compare the σ_{4d} for Pd in the metal and in Pd_2Si (Fig. 8). In this case, the $4d$ states are involved in the formation of bonding and antibonding hybrids with the Si $3p$ valence states.[27,29,39,40] The comparison is therefore between $4d$-band-like states with different chemical hybridizations (d-d overlap in the metal and d-p mixing in the silicide). A strong modification of σ is therefore not

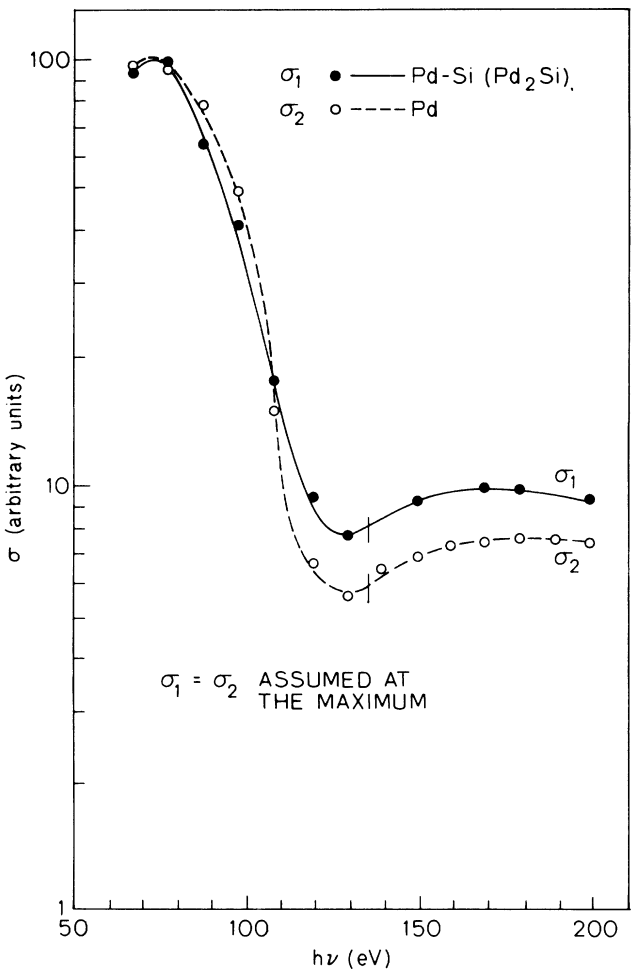

FIG. 8. Experimental σ for the $4d$ subshell of Pd in Pd metal (thick film) (dashed line) and at the Pd/Si interface as prepared by evaporating 4 ML of Pd onto Si(111) 2×1 to produce a Pd_2Si-like layer. The σ curves were arbitrarily normalized at the maximum for graphical convenience.

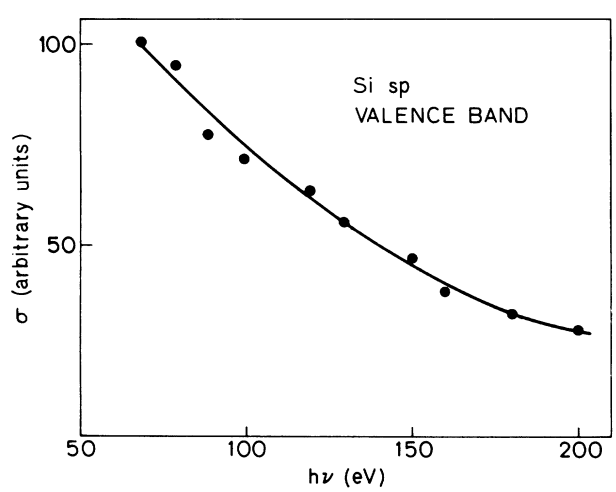

FIG. 9. Experimental σ for the $n=3$ shell of Si (sp) (linear plot).

expected in this case. This is strongly confirmed by the σ of Fig. 8 for Pd and Pd_2Si (normalized at the maximum as usual). The difference between the two σ's is small, taking into account the error bars and the uncertainty in the background subtraction, but has significantly opposite signs with respect to the previous cases. The CM for the $4d$ states in Pd_2Si is *smaller* than that of the metal, due to the decreased d character of the hybridized states.

On the basis of the presented data, we have shown that the cross section for photoionization in the Cooper-minimum region is very sensitive to the nature of the $4d$ and $5d$ initial states, and therefore σ measurements in solids yield information on the hybrid (bandlike) or atomiclike character of d valence states in compound alloys and interfaces.

V. APPLICATIONS TO SOLID-STATE ELECTRON SPECTROSCOPY

The presence of modulations in the cross section for photoionization over a photon-energy range covered by available sources relevant for solid-state electron spectroscopy (surface sensitivity and final states in the continuum) can be exploited with great advantage, particularly in the study of compounds and interfaces.

In this section we present results on solid systems which show the generality of the trends of σ discussed above and indicate how, even at the present state of only qualitative understanding of this new research field, one can obtain insights on the nature of the chemical bonds in solids.

The systems discussed all belong to the elemental semiconductor—transition-metal kind. These systems are particularly suitable for $h\nu$-dependent photoelectron spectroscopy because of the strong variability of $\sigma_{4d,5d}$ as opposed to the small changes in the $\sigma_{\mathrm{Si}\,3sp}$ or $\sigma_{\mathrm{Ge}\,4sp}$ valence states. It was actually the need to understand the nature of the valence states in Pd silicides that stimulated the use of photoemission at the CM as a way to gain sensitivity to the Si-originated valence states in the silicides, otherwise obliterated by the much higher intensity for the Pd $4d$ emission at all the $h\nu$ values far from the CM. All the above and following considerations, however, can be generalized, and the material presented here is only one example of CM effects in partial photoionization cross sections.

A. Cooper-minimum spectroscopy

The difficulty of conventional UPS with laboratory light sources in studying transition-metal silicides or semiconductor—transition-metal interfaces is related to the fact that at the low photon energies the σ_{4d} or σ_{5d} are much higher than the σ_{3s},σ_{3p} of Si or σ_{4s},σ_{4p} of Ge. As a result, the photoemission EDC's are dominated by strong features due to the emission from the d states, and all the information relative to the semiconductor originated states is lost in the background.

By tuning monochromatized SR to the Cooper minimum for the d emission, one obtains EDC's that are equally sensitive (see above) to d and non-d states. Therefore, the semiconductor s and p contributions to the total DOS become observable, and the electronic structure of

the compound can be understood on a pure experimental basis.

As introduced above, Figs. 4 and 5 show valence band EDC's for Pd, Pt, Ag, Au and for their reaction products with Si (Ge) at the interfaces. The solid curves were obtained with light of $h\nu=80$ eV; this value falls in all cases in the maximum region of σ_{4d} (see Figs. 6 and 8) and σ_{5d} (see Fig. 7).

At this energy, the σ_{sp} for Si is 1 order of magnitude smaller, so that curves A and A^1 in both figures show EDC's that describe the sole distribution of the d valence states in those materials. The curves B and B^1 (dashed-dotted) are EDC's obtained with $h\nu=130$ eV in the CM region for σ_{4d} and σ_{5d} (see Figs. 6 and 8). Here the σ_{sp} for Si and Ge is of comparable value to the $\sigma_{4d,5d}$, and the spectra indeed show the details of the Si contributions. The analysis of these Si-derived structures and of the metal derived structures has led to a satisfactory understanding of the near-noble-metal silicides[27,18,20] and the Si-Au, Ge-Au alloys and Si/Ag, Ge/Ag interfaces chemical bonding structures.[19,32–35,41]

Of importance for the present discussion is the fact that, by subtracting CM EDC's from the non-CM EDC's, we obtain difference curves (bottom curves, dashed line, in Figs. 4 and 5) that are a good indicator of the energy distribution of the states of d symmetry in the valence band. In these difference curves, the sp contribution has been largely cancelled due to the small changes in the σ_{sp} between 80 and 130 eV compared to the change in the σ d. Therefore, the difference between these difference curves and the pure metal d DOS are an indicator of the redistribution in energy and rehybridization of the d states in the compound or interface phase. A clear example is that of the Pt/Si interface, characterized by a Pt-rich mixed phase (see Ref. 20). The difference curve A-B strongly differs from the metal d-dominated EDC and also from the Pd-Si d-dominated EDC at $h\nu=80$ eV. These two facts carry information on both the new energy distribution of d states and on the distortion of the d wave function for different states in the compound which is also reflected in the different σ curves for states with different binding energies. This last point will be clarified in the next section.

Besides obtaining direct information on the valence states, this method and the difference curves give a valuable input to the theory. Partial DOS calculations can be directly compared with experimental "partial" DOS to achieve better agreement and understanding than otherwise obtainable on the basis of total DOS calculations and d-dominated EDC's. As an example, we propose the partial 5d DOS for Au in Au_3Si calculated with a semiempirical method[35] compared to our experimentally determined difference curve for Au 5d states at the Au/Si interface (Fig. 10).

B. Full-range $h\nu$-dependent photoemission

Observing the valence band spectra for the d metals in Figs. 4 and 5 (top curves), it can be noted that the CM EDC's are also different in shape, besides intensity, with respect to the non-CM (80-eV) curves. Owing to the rather flat[40] distribution of p- and s-metal valence states, the difference in shape is due to different σ dependence of the photoemission from d states that have different binding energies.

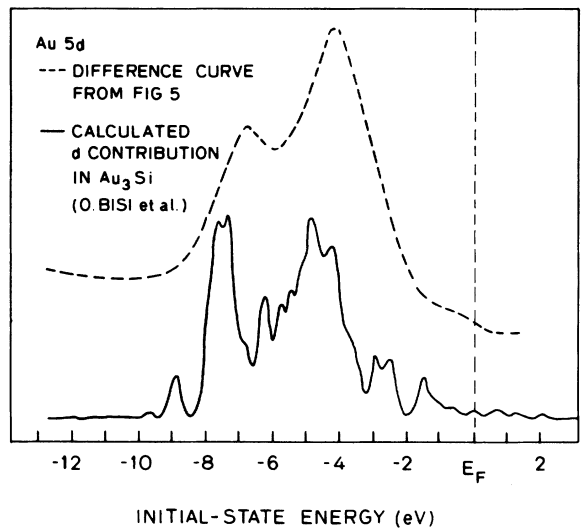

FIG. 10. Comparison between the 5d partial contribution to the valence emission of Au in the Au/Si interface from Fig. 4 (dashed curve) and theoretical 5d partial density of states in Au_3Si from Ref. 40 (see text).

We will not discuss here the branching ratio effect in Au 5d or Ag 4d for which exists a large literature, although no final explanation for the phenomenon has been achieved. It is possible to identify in Pt and Pd regions of the d band that indicate different σ values. We present such analysis for the bonding and antibonding states of Pd

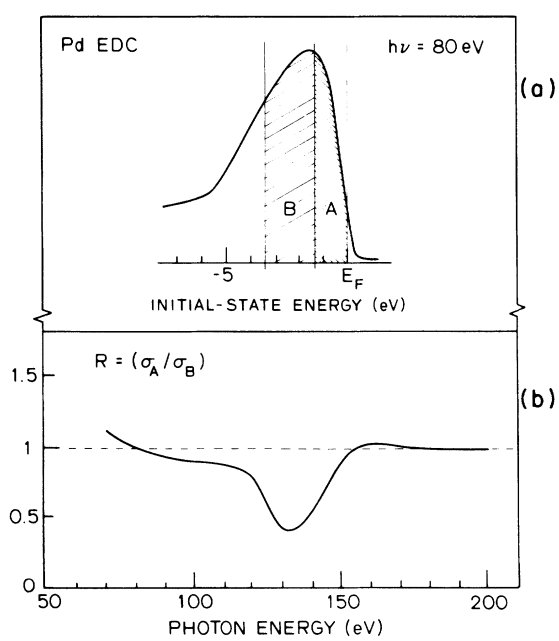

FIG. 11. (a) Schematic division of 4d bonding (B) and antibonding (A) valence states in metallic Pd. (b) Ratio between the σ curves obtained for the regions A and B of the 4σ band of Pd. The structure in the $R=\sigma_A/\sigma_B$ curve indicates that at the Cooper minimum energies the σ for antibonding states has a more pronounced CM (atomiclike) than the σ for bonding states.

in Fig. 11, where we plot the C for regions A and B of the valence band (being a comparison between states of the same band of the same sample, it can be done directly on the counting rates, avoiding the corrections and relative uncertainties in transforming C to σ). The limits of regions A and B are arbitrary. The location of the antibonding states agrees with the theory, while the bonding states extends below our limit at 3.5 eV below E_F. This limit is necessary because, for lower initial-state energies, the subtraction of the experimental background becomes uncertain. The two C curves show the presence of a difference in the two σ's. The bonding states seem to suffer the solid-state effect more strongly than the antibonding. A full discussion of this point is not possible at present and will require a theoretical investigation which we hope to stimulate. It is, nevertheless, clear that the σ is extremely sensitive to the details of the "chemical" nature of the initial-state wave function, and that, in general, d states heavily involved in bonding configurations present smaller σ modulations and a smaller CM than more atomiclike d states.

C. One application: The Si/Mo interface

A very convincing application of the above argument is the study of the Si/Mo interface that, for thin Mo overlayers, is characterized by a mixed phase.[21,42] The EDC for this mixed phase is given in Fig. 12 for a sample prepared by depositing 10.5 ML of Mo onto Si(111), as obtained with photon energies between 70 and 200 eV. The changes in the shape of the Si/Mo EDC are dramatic so that the interpretation of one of these EDC's independently from the others would be extremely misleading. Two regions in the EDC's can easily be identified as having "stability" of the spectroscopic features over the $h\nu$ range. The region of the shallow states A and that of the deeper states B are defined in the inset of Fig. 13, and the measured σ_A and σ_B are plotted. A difference factor of 5 in the σ^* at the CM is present between σ_A and σ_B, with the shallow states having a more atomiclike Cooper effect. The reduction values at the CM for these curves should not be quantitatively compared with those relative to the corrected σ in Sec. V A of this paper. Figure 13 is a plot

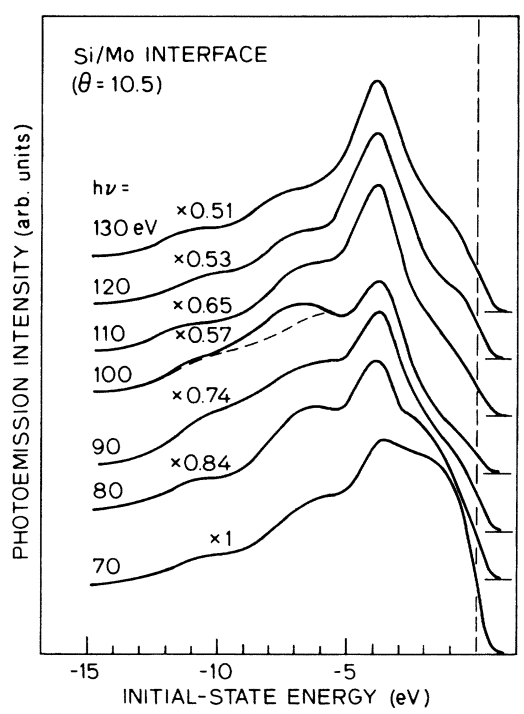

FIG. 12. Angle-integrated electron-energy distribution curves for the valence states at the Si/Mo interface as prepared by evaporating 10.5 ML of Mo onto Si(111) 2×1. EDC's taken at $h\nu$ values between 70 and 120 eV are shown and the magnification factor used to plot curves of the same amplitude is indicated. The dashed line on the curve obtained with $h\nu=100$ eV indicates a region of emission due to the presence of the Si LVV Auger line at ~91 eV of kinetic energy. The shallow states between -5 eV and E_F are dominated by the $4d$ emission of Mo that has much higher σ than the Si originated states.

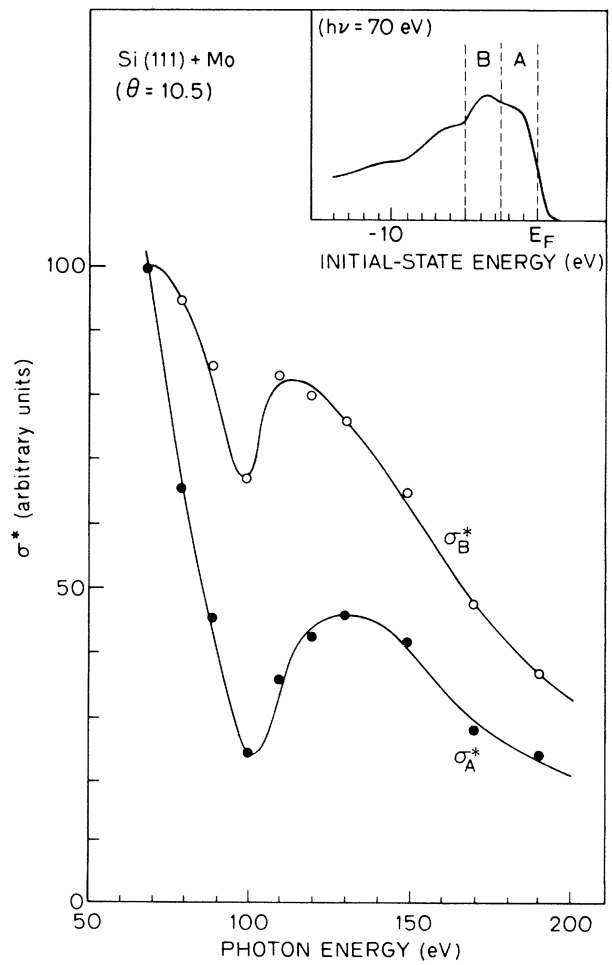

FIG. 13. Experimental uncorrected σ^* for two regions of Mo $4d$ states at the Si/Mo interface. σ_A^* and σ_B^* are plotted, and the boundaries between the two sets of states are indicated on the EDC in the top panel. The σ^* for the states between -5 and -2.5 eV below E_F shows a smaller modulation in the Cooper-minimum region indicating that these states are largely involved in the bonding configuration. Being a comparison between σ^* of states of the same electronic structure of the same sample, the optical corrections are not necessary because all the optical effects are cancelled out in the comparison.

of uncorrected σ^*. As noted above, this fact is not important when we compare σ^*'s for the *same* sample. The smaller CM effect for the deeper states (B) cannot be due to the presence of a stronger Si background contribution because Si valence states have a σ 1 order of magnitude smaller than that for Mo $4d$.[12,43] This contribution can smooth the curve but cannot originate the effect. The difference between σ_A and σ_B is therefore not affected by artifacts and can be interpreted as the direct experimental evidence that in Si-Mo the shallow d states are "atomiclike," i.e., little involved in the bond or nonbonding. This is in agreement with the theory of the DOS in the silicon—refractory-metal silicides.[44] It has, in fact, been proposed that the strong metal—metal bonds typical of bulk Mo are broken so that a part of the d states is involved in bonds with Si, and another part is of nonbonding character in the Fermi-level region.

The present cross-section results are the most direct and convincing experimental proof of this scheme for the DOS of Mo-Si. We stress that these conclusions on the nature of the d states in Si-Mo were reached on a mere experimental basis by applying the considerations on σ presented in this paper. This is a very important point because our method can be used to understand the physics of systems for which significant calculations are unavailable or impossible.

VI. CONCLUSIONS

We have presented photoionization cross sections for a variety of $4d$ and $5d$ metals, compounds, and interfaces. A solid-state effect is present on the σ and has been discussed at a phenomenological level stressing the importance of the changes of the initial-state wave functions in going from the atomiclike to the solid state and at the solid state from band character due to d-d overlapping to the rehybridized character due to orbital mixing with states of non-d nature.

We demonstrated the existence of such effects with a variety of examples relative to known systems, and we finally showed how to apply cross-section considerations to the spectroscopic study of unknown electronic structures (like the Si/Mo system) and the important information that can be obtained from this approach.

ACKNOWLEDGMENTS

Our work has greatly benefited from suggestions and comments by Mike Hecht, whose thesis work includes an extensive description and evaluation of experimental σ determinations in the solid state. This work was supported by the Gruppo Nationale di Struttura della Materia del Consiglio Nationale delle Ricerche, Italy, and by the U. S. Navy Office of Naval Research under Contract No. N00014-82-K-0524. The experiments were performed at the Stanford Synchrotron Radiation Laboratory which is supported by the U. S. Department of Energy, Office of Basic Energy Sciences, and the National Science Foundation, Division of Materials Research.

[1]J. W. Cooper, Phys. Rev. 128, 681 (1962).
[2]U. Fano and J. W. Cooper, Rev. Mod. Phys. 40, 441 (1968).
[3]S. T. Manson and J. W. Cooper, Phys. Rev. 165, 126 (1968).
[4]G. M. Bancroft, W. Gudat, and D. E. Eastman, Phys. Rev. B 17, 4499 (1978).
[5]S. Suzer, P. R. Hilton, N. S. Huch, and S. Nordholm, J. Electron Spectrosc. Relat. Phenom. 12, 357 (1977).
[6]S. P. Shannon and K. Codling, J. Phys. B 11, 1193 (1978).
[7]L. I. Johansson, I. Lindau, M. H. Hecht, and E. Kallne, Solid State Commun. 34, 83 (1980).
[8]M. Hecht and I. Lindau, Phys. Rev. Lett. 47, 821 (1981).
[9]I. Abbati, L. Braicovich, G. Rossi, I. Lindau, U. del Pennino, and S. Nannarone, Phys. Rev. Lett. 50, 1799 (1983).
[10]G. Rossi, J. J. Yeh, M. Hecht, L. Braicovich, and I. Lindau (unpublished).
[11]I. Lindau, P. Pianetta, and W. E. Spicer, Phys. Lett. A 57, 225 (1976).
[12]S. M. Goldberg, C. S. Fadley, and S. Kono, J. Electron Spectrosc. Relat. Phenom. 21, 285 (1977).
[13]M. H. Hecht, Ph.D. thesis, Stanford University, 1982 (unpublished).
[14]P. Pianetta, I. Lindau, and W. E. Spicer, *Quantitative Surface Analysis of Materials, Cleveland, 1977,* edited by N. S. McIntyre (American Society for Testing and Materials, Philadelphia, 1978), p. 105.
[15]P. W. Palmberg, J. Vac. Sci. Technol. 12, 379 (1975).
[16]F. C. Brown, R. Z. Bachrach, and N. Lien, Nucl. Instrum. Methods 152, 73 (1978).
[17]M. H. Hecht and I. Lindau, Nucl. Instrum. Methods 195, 339 (1982).
[18]I. Abbati, G. Rossi, L. Braicovich, I. Lindau, and W. E. Spicer, J. Vac. Sci. Technol. 19, 636 (1981).
[19]G. Rossi, I. Abbati, L. Braicovich, I. Lindau, and W. E. Spicer, Phys. Rev. B 25, 3619 (1982).
[20]G. Rossi, I. Abbati, L. Braicovich, I. Lindau, and W. E. Spicer, Phys. Rev. B 25, 3627 (1982).
[21]G. Rossi, I. Abbati, L. Braicovich, I. Lindau, W. E. Spicer, U. del Pennino, and S. Nannarone, in *Proceedings of the 16th International Conference on the Physics of Semiconductors,* edited by M. Averous (North-Holland, Amsterdam, 1983) [Physica B 117 and 118 (1983)], pp. 795—797.
[22]B. H. Henke, Phys. Rev. A 6, 94 (1972).
[23]L. I. Johansson, I. Lindau, M. H. Hecht, S. M. Goldberg, and C. S. Fadley, Phys. Rev. B 20, 4126 (1979).
[24]M. P. Seah and W. A. Dench, Surf. Interface Anal. 1, 2 (1979).
[25]P. S. Ho, P. E. Shmidt, and H. Foll, Phys. Rev. Lett. 46, 782 (1981).
[26]I. Lindau and W. E. Spicer, J. Electron Spectrosc. Relat. Phenom. 3, 409 (1974).
[27]G. Rossi, I. Abbati, L. Braicovich, I. Lindau, and W. E. Spicer, Solid State Commun. 39, 195 (1981).

[28]I. Abbati, G. Rossi, L. Braicovich, I. Lindau, and W. E. Spicer, Appl. Surf. Sci. 9, 243 (1981).

[29]For reviews, see G. W. Rubloff and P. S. Ho, in *Thin Films and Interfaces,* Vol. 10 of the *Materials Research Society Symposia Proceedings,* edited by P. S. Ho and K. N. Tu (North-Holland, New York, 1982); L. Braicovich, Thin Solid Films 104, 327 (1983).

[30]J. Stohr and R. Jaeger, J. Vac. Sci. Technol. 21, 619 (1982).

[31]A. McKinley, R. H. Williams, and W. A. Parke, J. Phys. C 12, 2447 (1979).

[32]G. Rossi, I. Abbati, L. Braicovich, I. Lindau, and W. E. Spicer, Surf. Sci. Lett. 112, L765 (1981).

[33]G. Rossi, I. Abbati, I. Lindau, and W. E. Spicer, Appl. Surf. Sci. 11/12, 348 (1982).

[34]L. Braicovich, C. M. Garner, P. R. Skeath, C. Y. Su, P. W. Chye, I. Lindau, and W. E. Spicer, Phys. Rev. B 20, 5131 (1979).

[35]O. Bisi, C. Calandra, L. Braicovich, I. Abbati, G. Rossi, I. Lindau, and W. E. Spicer, J. Phys. C 15, 4707 (1982).

[36]J. N. Miller, S. A. Swartz, I. Lindau, W. E. Spicer, B. de Michelis, I. Abbati, and L. Braicovich, J. Vac. Sci. Technol. 17, 920 (1980).

[37]M. S. Banna, M. O. Krause, and F. Wuilleumier, J. Phys. B 12, L125 (1979).

[38]See, for example, *Photoionization and Other Probes of Many Electron Interactions,* edited by F. J. Wuilleumier (Plenum, New York, 1976).

[39]G. W. Rubloff, P. S. Ho, J. F. Freeouf, and J. E. Lewis, Phys. Rev. B 23, 4183 (1981).

[40]O. Bisi and C. Calandra, J. Phys. C 14, 5479 (1981).

[41]P. Perfetti, G. Rossi, I. Lindau, and O. Bisi, Surf. Sci. Lett. 124, L19 (1983).

[42]G. Rossi, I. Abbati, L. Braicovich, I. Lindau, and W. E. Spicer, J. Vac. Sci. Technol. 21, 617 (1982).

[43]J. J. Yeh (unpublished).

[44]A. Franciosi, J. H. Weaver, J. G. O'Neill, Y. Chabal, J. E. Rowe, J. M. Poate, O. Bisi, and C. Calandra, J. Vac. Sci. Technol. 21, 264 (1982).